Basili R. and S. Barba (2007). Migration and shortening rates in the northern Apennines, Italy: implications for seismic hazard. Terra Nova 19 (6), 462–468. doi:10.1111/j.1365-3121.2007.00772.x

Migration and shortening rates in the northern Apennines, Italy: implications for seismic hazard

Roberto Basili and Salvatore Barba

Istituto Nazionale di Geofisica e Vulcanologia
Sezione di Sismologia e Tettonofisica
Via di Vigna Murata, 605 - 00143 Rome, Italy

Corresponding author:
Roberto Basili
e-mail: roberto.basili@ingv.it
Phone: +390651860516
Fax: +39065041181

Short title: Migration and shortening rates in the Apennines

To cite this article:
Basili R. and S. Barba (2007). Migration and shortening rates in the northern Apennines, Italy: implications for seismic hazard. Terra Nova 19 (6), 462–468. doi:10.1111/j.1365-3121.2007.00772.x

Abstract: Is compression across the northern Apennine fold-and-thrust system (Italy) still active? To address this question we quantified the long-term rates of migration and shortening of the system along with the measurement errors. Our approach integrates structural geology, seismicity patterns, and statistical treatment of tectonic activity. Based on recently published surface and subsurface data, we found a migration rate of **8.85+/-0.61 mm/y**. The inception age of individual fold structures follow closely this average rate, indicating that the system has been migrating at a constant rate for the past 17 Myr. Cumulative shortening of the system also increases linearly through time at **2.93+/-0.31 mm/y**. The location of the youngest structures in the easternmost portion of the system coincides with a significant peak of seismic moment released by historical earthquakes. We conclude that not only these easternmost thrusts are still active, but also that they generate earthquakes.

Keywords: Active thrust faults, active folds, thrust belt migration, shortening, earthquakes.

1 – Introduction

NE-verging folds and thrusts, developed throughout the Neogene (ca. 20 Myr), dominate the structural architecture of the northern Apennines (**Figure 1, 2**). Abundant geological literature describes these structures in fine detail and broad agreement exists on the fact that the fold-and-thrust system migrated progressively north-eastward. However, diverging opinions stir up the debate on the present-day activity of the easternmost structures. Based on the interpretation of conventional seismic profiles, many authors conclude that compression ended in the Middle Pleistocene [e.g. *Argnani and Gamberi*, 1997; *Coward et al.*, 1999; *Di Bucci and Mazzoli*, 2002] and was replaced by extension [e.g. *Bertotti et al.*, 1997; *Di Bucci et al.*, 2003]. However, compressional earthquakes occur along the Apennine foothills [e.g. *Frepoli and Amato*, 1997; *Vannucci et al.*, 2004; *Piccinini et al.*, 2006] and many authors maintain they can be related to the still active thrusting [e.g. *Negredo et al.*, 1999; *Carminati et al.*, 2003; *Montone et al.*, 2004; *Vannoli et al.*, 2004; *Scrocca*, 2006; *Lavecchia et al.*, 2007; Scrocca et al., 2007]. This debate has significant seismic hazard implications because the active structures at the Apennine foothills are buried under lowland where population, industrial activities, and critical facilities concentrate, and where large historical earthquakes had occurred.

Relating seismicity to geological structures in our study area is not straightforward because the subsurface geology and the seismic network geometry make the single hypocenter depths unreliable. We thus treat earthquakes collectively and rely on average depths. In **Figure 3**, we compare two 90-km-wide swath profiles of the seismic moment released by historical earthquakes [*Gruppo di Lavoro CPTI*, 2004] and by instrumental earthquakes [*Chiarabba et al.*, 2005]. The 100-fold exaggeration on the instrumental moment scale compensates the time-span ratio with the historical catalogue (20 yr vs. ~2000 yr) and allows comparing the rates of seismic release (the historical rate is underestimated because the catalogue is complete for M4.9 only for the last 500 years). Seismicity concentrates in three sectors at -80, -50, and -10 km from the Offshore Anticline axis. In those three sectors the seismic release occurs at different average depths and with different mechanisms; from SW to NE, the effective depth is 8-12, 12-20, 5-8 km, whereas the average faulting mechanism is normal, possibly compressive, and compressive (**Figure 1, 2**). At -80 km, the historical and instrumental releases almost coincide. At -50 km, the historical moment may be overestimated due to hypocenter depths underestimation. At -10 km, the peak from instrumental earthquakes does not match that from the historical earthquakes, hinting at a significant lack of seismic release in recent times.

The purpose of this paper is to investigate and gain insight on the present-day deformation of the easternmost sector of the northern Apennines from its long-term tectonic history. To this end, we develop a novel approach that integrates structural geology, seismicity analysis, and statistical predictions of tectonic activity. We also accompany our analysis with detailed error estimates. Our procedure will thus allow scientists to reproduce our results and carry out additional analyses in Italy or in similar tectonic environments elsewhere. We use data from the CROP03 project [*Pialli et al.*, 1998] to analyze the activity migration and the shortening evolution of the contractional belt. Special attention is given to a structural layer - very well imaged by seismic reflection profiles - made up by high-rigidity Mesozoic rocks deformed by thrust faults whose size is typical of potential sources of significant earthquakes (M~6; **Figure 1, 2**).

2 – Available data from the CROP03 profile

The CROP03 project [*Pialli et al.*, 1998] lasted about five years, involved more than one hundred people, and produced a wealth of original, good-quality data. According to *Barchi et al.* [1998], the fold-and-thrust system of the Umbria-Marche Apennines has three major structural layers (**Figure 2**): (1) "Shallow Embricates" (SE), which extends from 0 to 2 km depth, is characterized by structures with a wavelength of a few hundreds meters, and hosts the so called "out of sequence" structures that developed on a detachment located above the Jurassic-Cretaceous Carbonates; (2) "Umbria-Marche Folds" (UMF), which extends down to 6-10 km depth and is characterized by structures with a wavelength of 5-10 kilometers that developed on a detachment located within the Triassic Evaporites Formation; and (3) "Basement Wedges", which extends below the UMF, characterized by structures with a wavelength of 25-35 kilometers that affect the entire upper and lower crust.
The UMF layer comprises seven folds (from SW to NE, **Figure 2**): Perugia Massif (PM), Gubbio Anticline (GA), Inner Ridge (IR), Outer Ridge (OR), Mondaino Anticline (MA), Coastal Anticline (CA), and Offshore Anticline (OA). The syntectonic deposits, i.e. the Neogene turbidites, constrain the age of activity of each structure. **Table 1** shows the time history of the fold-and-thrust system. We use the geochronological ages of fold activity from *Barchi et al.* [1998], *Barchi et al.* [2001], *Argnani* [1998], *De Donatis et al.* [1998], *Coward et al.* [1999], and *Di Bucci and Mazzoli* [2002]. Numerical ages were assigned based on the geological time scale by *Gradstein et al.* [2004].

3 – Space-time contractional evolution

Based on the data summarized in **Table 1**, we calculated the rate at which the tectonic activity in the Umbria-Marche Apennines migrates north-eastward while generating the fold-and-thrust system within the UMF structural layer. To this end, we calculated the apparent migration rate (age of activity relative to present distance) and the shortening rate of the system and then combined the two results to obtain the true migration rate (age of activity relative to distance plus shortening). The Plio-Quaternary extensional deformation of the inner Apennines was restored before taking the measures (**Figure 2**).

The apparent migration was computed through least-squares regression of inception ages on distance of folds. We estimated errors on age as being equal to half duration of the geologic time interval and errors on distance equal to the maximum horizontal fluctuation of fold axes. **Figure 4** shows that a straight line fits properly the time history with little scattering of data suggesting that migration of activity progressed rather regularly from trailing to leading structures. The apparent average rate of migration of the fold-and-thrust tectonic activity is **5.92+/-0.30 mm/y**. In **Figure 4** we also show that different datasets of inceptions and terminations run almost parallel to the regression line indicating that our results do not depend much on whether inceptions or terminations are used. However, *Brozzetti et al.* [2002] set the inception of the PM fold in the middle-late Serravallian implying that the average velocity might be slightly faster.

To measure the amount of progressive shortening in the UMF structural layer, we restored the CROP03 section in seven successive steps, one for each fold. A "pin line" was placed in front of the easternmost and youngest anticline and a "loose line" was placed in front of each older structure (**Figure 2**). Each step gave a measure of the shortening increment. We assume that the geometry of the *Barchi et al.* [1998] profile is correctly

balanced and well represents the entire structure under analysis and that age constraints are reliable.

To calculate the shortening rate, we first measured the amount of line-length shortening for three key layers: the Fucoids Marls (FM), the top of the Evaporites (TE), and the top of the Basement (TB). We also quantified the errors affecting the key reflectors length: a) uncertainty in the reflector position (1/2 physical thickness of reflectors in the seismic line); b) velocity model (3% of depth of reflectors); c) discretization error (1/2 thickness of reflectors in the line drawing); d) possible recumbent portion of folds not drawn in the section (measuring the hidden area below the fold and assuming an average fold dip of 20°). The maximum possible error (**Table 1**) were calculated by considering that shortening is overestimated by a) and b), and is underestimated by a), b), c), and d). The maximum underestimation on the total is ~9 km. For each fold, we consider as our best shortening estimate the measured values plus one-half of the bias given by c) plus d). Assuming uniform probability (not Gaussian) of the true measurement of the fold shortening inside our error band, we compute the 2σ error (95.44% confidence) on the cumulative shortening. We also tried to calculate shortening using the area method but found that propagating the uncertainty on the detachment depth throughout this long section leads to an unbearable overall uncertainty. We then calculated a least-squares regression of all observations vs. space including replicates (one shortening value per key layer). This approach assumes that the shortening values obtained for the three key layers are significant samples of a normally distributed (Gaussian) population - as if shortening were measured along several layers - and the scatter in the data is entirely due to the interaction between the rheological properties of rocks and the physical process of deformation. **Figure 5a** shows the cumulative shortening vs. distance covered through apparent migration. A straight line fits appropriately the data points with low residuals, suggesting that the entire system shortens at a rather constant rate. The best-fitting line gives a ratio of shortening over apparent migration distance of **0.49+/-0.03.** By multiplying the shortening ratio over space by the apparent migration rate we obtained the shortening rate of **2.93+/-0.31 mm/y**.

We tested the regression through the analysis of variance at **5%** significance level. The *F*-tests yielded $\boldsymbol{F=539.51}$ for the goodness of fit, and $\boldsymbol{F=4.83}$ for the appropriateness of the straight-line model. The first *F* value is largely greater than that tabulated ($\boldsymbol{F_{.05}(1,19)=4.38}$ using conventional notation), indicating that the fit is robust and reliable despite the relatively small number of observations. Therefore, we expect the conclusions not to change significantly if analysis of different cross sections or future data would be included; we would rather expect uncertainties to reduce. The second *F* value is slightly bigger than that tabulated ($\boldsymbol{F_{.05}(5,14)=2.96}$) but still rather small (commonly, a significant lack of fit deserves attention when $\boldsymbol{F>>1}$). This lack of fit depends on the GA that is crossed by the section in an unfavorable position; removing this outlier improves the fit enormously. Therefore we consider that the straight-line model is adequate and the use of more complex functions is not justified. For comparison we also show (**Figure 5b**) the cumulative shortening vs. time of growth termination of carbonate anticlines (**Table 1**). Using the termination age of "out of sequence" shallow thrusting also gives similar results, although with more scatter. With the data at hands it was not possible to estimate how much shortening occurs within the UMF layer during the "out of sequence" thrusting as described in *Barchi et al*. [1998]. However, combining migration and shortening over distance of the final position of folds allowed us to overcome this problem. This method only applies when the activity intervals of adjacent folds overlap (**Figure 4**), otherwise only the times of termination should be used.

In addition, considering that the geometry of the FM and TE reflectors is more reliable than the deeper and more questionable portion of the section, we show that including or excluding the data on TB yields similar linear fits (**Figure 5**).

Finally, by combining apparent migration and shortening we obtained a true migration rate of **8.85+/-0.61 mm/y**. **Figure 6** shows our comprehensive model for linear migration and shortening.

4 – Discussion and conclusion

Within the limits of reliability of the available data, our results indicate that compression in the northern Apennines must be driven by long-lived (>17 Myr) and constantly migrating tectonic forces. Thrust migration in the Apennines is strictly linked to the ongoing geodynamic process [*Doglioni*, 1991]; therefore, the rates of migration and shortening can be used for constraining geodynamic modeling or simulations at the same scale of ours (~10-100 km, ~0.5-20 Myr). They will also be useful for comparison with other sectors of the Apennines and other contractional belts worldwide.

How does the identified geological trend compare with the seismological evidence for fault activity? In **Figure 3** we outlined three parallel sectors that agree fairly well with previous tectonic schemes [e.g. *Doglioni*, 1991; *Lavecchia et al.*, 1994]. Interestingly, the easternmost sector spans almost exactly the area of CA and OA. In addition, instrumental seismicity in this area occurs in the same depth range as the thrust faults of the UMF layer and the stress field orientation [see also *Montone et al.*, 2004] favors their reactivation. This sector also includes the largest and most damaging historical earthquakes of the Apennine foothills (e.g. M5.9 Rimini, 1916; M5.9 Senigallia, 1930). These observations support the thesis that not only CA and OA are active, as suggested by the long-term evolution of the belt, but also seismogenic. In other words, if the seismic moment deficit in the coastal sector (**Figure 3**) has to be compensated, the faults cutting the high-rigidity Mesozoic rocks and controlling the growth of the CA and OA folds are our favorite candidates to do the work.

We conclude that the tectonic process controlling the build up of the entire northern Apennines has been going ahead for about 17 Myr with fluctuations of activity of individual structures that, in most cases, are within errors. Our statistics along with error estimates predicts that the thrust system is still active. However, the deformation rate is very slow (from the CROP03 the tilt rate of fold forelimbs is $2x10^{-6}$-$1x10^{-5}$ deg/y, yielding only 2-8 deg tiling of Middle Pleistocene deposits) and we do not know what fraction goes aseismic. *Vannoli et al.* [2004] calculated that one thrust fault associated with CA has a Late Pleistocene slip rate of 0.24-0.36 mm/y and maintain that the youngest blind thrust faults produce very subtle deformation. *Scrocca et al.* [2007] suggest that the scarce evidence of deformation is related to the larger sediment input into the foredeep-piggy-back basin with respect to slip rate. They also suggest a shortening deceleration during the Quaternary based on the larger loading of the accretionary prism [*Carminati et al.*, 2004]. We therefore disagree with those views that suggest that the thrust belt has not been active since the Middle Pleistocene. In terms of seismic hazard implications, our results indicate that the coastal and offshore anticlines deserve the most attention to establish more firmly their seismogenic potential.

Acknowledgments

Thanks go to Regione Marche for financial support, to G. Valensise for backing us up throughout the preparation of the manuscript, and to G. Vannucci for elaborations with the EMMA database. A. Argnani, M.R. Barchi, and G. Cello made critical reviews that significantly improved the paper.

Reference list

Argnani A. (1998), Structural elements of the Adriatic foreland and their relationships with the front of the Apennine fold-and-thrust belt, *Mem. Soc. Geol. It.*, **52**, 647-654.

Argnani, A., and F. Gamberi (1997), Stili strutturali al fronte della catena appenninica nell'Adriatico centro-settentrionale, *Studi Geologici Camerti*, Volume Speciale 1995/1, 19-27.

Barchi, M. R., A. De Feyter, M. B. Magnani, G. Minelli, G. Pialli, and B. M. Sotera (1998), The structural style of the Umbria-Marche fold and thrust belt, *Mem. Soc. Geol. It.*, **52**, 557-578.

Barchi, M., A. Landuzzi, G. Minelli, and G. Pialli (2001), Outer Northern Apennines. In: Anatomy of an Orogen: the Apennines and adjacent Mediterranean basins (G. B. Vai and I. P. Martini, eds) Kluwer Academic Publishers, UK, 215-254.

Bertotti, G., R. Capozzi, and V. Picotti (1997), Extension controls Quaternary tectonics, geomorphology and sedimentation of the N-Apennines foothills and adjacent Po Plain (Italy), *Tectonophysics*, **282**, 291-301.

Brozzetti, F., P. Boncio, and G. Pialli (2002), Early-middle Miocene evolution of the Tuscan Nappe–western Umbria foredeep system: insights from stratigraphy and structural analysis, *Bull. Soc. Geol. It.*, spec. vol. 1, 319-331.

Carminati, E., C. Doglioni, and D. Scrocca (2003), Apennines subduction-related subsidence of Venice (Italy), *Geophys. Res. Lett.*, **30**, 13, 1717, doi:10.1029/2003GL017001.

Carminati E., C. Doglioni, and S. Barba (2004), Reverse migration of seismicity on thrusts and normal faults, *Earth Science Reviews*, **65**, 195-222.

Chiarabba, C., L. Jovane, and R. Di Stefano (2005), A new view of Italian seismicity using 20 years of instrumental recordings, *Tectonophysics*, **395**, 251-268.

Coward, M. P., M. De Donatis, S. Mazzoli, W. Paltrinieri, and F. C. Wezel (1999), Frontal part of the northern Apennines fold and thrust belt in the Romagna-Marche arc (Italy): shallow and deep structural styles, *Tectonics*, **18**, 559-574.

De Donatis, M., C. Invernizzi, A. Landuzzi, S. Mazzoli, and M. Potetti (1998), CROP 03: Structure of the Montecalvo in Foglia-Adriatic Sea segment, *Mem. Soc. Geol. It.*, **52**, 617-630.

Di Bucci, D., and S. Mazzoli (2002), Active tectonics of the Northern Apennines and Adria geodynamics: new data and a discussion, *Journal of Geodynamics*, **34**, 687-707.

Di Bucci, D., S. Mazzoli, O. Nesci, D. Savelli, M. Tramontana, M. De Donatis, and F. Borraccini (2003), Active deformation in the frontal part of the Northern Apennines: insights from the lower Metauro River basin area (northern Marche, Italy) and adjacent Adriatic off-shore, *Journal of Geodynamics*, **36**, 213-238.

Doglioni, C. (1991), A proposal of kinematic modelling for W-dipping subductions - Possible applications to the Tyrrhenian - Apennines system, *Terra Nova*, **3**, 423-434.

Frepoli, A., and A. Amato (1997), Contemporaneous extension and compression in the Northern Apennines from earthquake fault-plane solutions, *Geophys. J. Int.*, 129 (2), 368-388.

Gradstein, F. M., J. G. Ogg, A. G. Smith, W. Bleeker, and L. J. Lourens (2004), A new Geologic Time Scale, with special reference to Precambrian and Neogene, *Episodes*, **27**, 83-100.

Gruppo di lavoro CPTI (2004), *Catalogo Parametrico dei Terremoti Italiani, versione 2004 (CPTI04)*, http://emidius.mi.ingv.it/CPTI/, INGV, Italy.

Lavecchia, G., F. Brozzetti, M. Barchi, M. Menichetti, and J. V. A. Keller (1994),

Seismotectonic zoning in east-central Italy deduced from an analysis of the Neogene to present deformations and related stress fields, *Geol. Soc. Am. Bull.*, **106**, 1107-1120.

Lavecchia, G., R. De Nardis, F. Visini, F. Ferrarini, and M. S. Barbano (2007), Seismogenic evidence of ongoing compression in eastern-central Italy and mainland Sicily: a comparison, *Boll. Soc. Geol. It. (Ital. J. Geosci.)*, **126**, 209-222.

Montone, P., M. T. Mariucci, S. Pondrelli, and A. Amato (2004), An improved stress map for Italy and surrounding regions (Central Mediterranean), *J. Geophys. Res.*, 109, B10410, doi:10.1029/2003JB002703.

Negredo, A. M., E. Carminati, S. Barba, and R. Sabadini (1999), Dynamic modelling of stress accumulation in central Italy, *Geophys. Res. Lett.*, **26**(13), 1945-1948.

Piccinini, D., C. Chiarabba, P. Augliera. and Monghidoro Earthquake Group (M.E.G.) (2006), Compression along the northern Apennines? Evidence from the Mw 5.3 Monghidoro earthquake, *Terra Nova*, 18, 89–94, doi: 10.1111/j.1365-3121.2005.00667.x.

Pialli, G., M. Barchi, and G. Minelli (Eds) (1998), *Results of the CROP03 deep seismic reflection profile*, Mem. Soc. Geol. It., **52**, 657 pp., Società Geologica Italiana, Rome, Italy.

Scrocca, D., (2006), Thrust front segmentation induced by differential slab retreat in the Apennines (Italy), *Terra Nova*, 18, 154–161, doi: 10.1111/j.1365-3121.2006.00675.x.

Scrocca D., E. Carminati, C. Doglioni, and D. Marcantoni (2007), Slab retreat and active shortening along the central-northern Apennines. In: Thrust belts and Foreland Basins: From Fold Kinematics to Hydrocarbon Systems, O. Lacombe, J. Lavé, F. Roure and J. Verges (Eds.), Frontiers in Earth Sciences, Springer, 471-487.

Vannoli, P., R. Basili, and G. Valensise (2004), New geomorphic evidence for anticlinal growth driven by blind-thrust faulting along the northern Marche coastal belt (central Italy), *Journal of Seismology*, **8**(3), 297-312.

Vannucci, G., and P. Gasperini (2004), The new release of the database of Earthquake Mechanisms of the Mediterranean Area (EMMA Version 2), *Ann. Geophys.*, Suppl. to Vol. 47 (1), 307-334.

Vannucci, G., S. Pondrelli, A. Argnani, A. Morelli, P. Gasperini. and E. Boschi (2004), An atlas of Mediterranean seismicity, *Ann. Geophys.*, Suppl. to Vol. 47, 247–306.

Figure 1 – (**A**) Main active tectonic features of the Northern Apennines along with average focal mechanisms from the EMMA database [*Vannucci and Gasperini*, 2004] and SHmin orientations [*Montone et al.*, 2004]. NATF: Northern Apennine Thrust Front; solid: generally accepted, dashed: from *Scrocca* [2006]. MAR: Mid Adriatic Ridge. AEB: Apennine Extensional Belt. TL: Tremiti Line. MGF: Mattinata-Gondola Fault. (**B**) Map of the study area. Squares: M>2.5 historical earthquakes [*Gruppo di Lavoro CPTI*, 2004]. Circles: instrumental earthquakes [*Chiarabba et al.*, 2005]. Dashed grey lines: anticline hinges [*Barchi et al.*, 1998; *Coward et al.*, 1999]. Solid grey line: CROP03 profile [*Pialli et al.*, 1998]. Dashed rectangle encloses the earthquakes used in **Figure 3**.

Figure 2 - NE-SW geological section across the Apennine fold-and-thrust belt from CROP03 data (modified from *Barchi et al.* [1998]; see **Figure 1** for location). PL: pin line; LL1-7: loose lines. The double-head arrow indicates the gross horizontal extension due to normal faulting.

Figure 3 - Swath profile (NE-SW) of the instrumental (100x) and historical scalar seismic moment released in the study area (enclosed in the dashed rectangle shown in **Figure 1**). Distance is from the axis of OA. The shaded areas indicate the three sectors with different faulting mechanisms and effective depths (shown in the upper part of the diagram). NF: normal faulting; TF: thrust/reverse faulting; Ze: effective depth. Notice that the seismic release from instrumental earthquake does not match the major peak from historical earthquakes indicating a seismic deficit across the CA and OA structures.

Figure 4 - Apparent migration of the Apennines fold-and-thrust system as derived from time of activity inception (see **Table 1**) of adjacent folds. Relevant periods of the geological time scale are shown on top of diagram for reference; bold lines indicate ages of "golden spikes" established by the International Stratigraphic Commission [*Gradstein et al.*, 2004]. Distance between successive structures is taken at the fold hinges (see **Figure 2**). The result of regression is shown inside the diagram. Age of inception and termination of growth of carbonate anticlines (UMF) and termination of "out of sequence" shallow thrusting (SE), as of *Barchi et al.* [1998], are also shown for comparison. Notice they describe a linear trend almost parallel to the regression line. Qualitative prospective termination ages of CA and OA are also shown.

Figure 5 - Cumulative shortening measured along the three key reflectors. (**A**) Shortening vs. distance taken at fold hinges (see **Figure 2**). (**B**) Shortening vs. time taken at the termination age of growth of carbonate anticlines (UMF) as of *Barchi et al.* [1998] (see **Table 1**). Results of regressions are shown inside diagrams along with the linear fit obtained without the data on TB.

Figure 6 – Linear model for shortening and migration (apparent and true) of the Northern Apennines.

Table 1 - Time history (**A**) and distance-shortening (**B**), along with measurement and 2σ cumulative errors, of the folds imaged in the CROP03 profile. ([1]) Ages averaged from *Argnani* [1998], *De Donatis et al.* [1998], *Coward et al.* [1999], and *Di Bucci and Mazzoli* [2002]; ([2]) ages from *Barchi et al.* [2001]; ([3]) ages from *Barchi et al*. [1998]. Termination ages are those of growth of carbonate anticlines (UMF) used in the regression shown in **Figure 5b**.

(A)	Inception			Termination		
Fold	Age	Ma	Err	Age	Ma	Err
OA	Late Pliocene – Early Pleistocene	2.2[1]	0.4	?	?	---
CA	Middle Pliocene	3.1[1]	0.5	?	?	---
MA	upper fourth of Messinian	5.8[3]	0.2	top Pliocene	1.8[3]	0.4
OR	early Messinian	6.9[2]	0.3	top Messinian	5.3[3]	0.3
IR	early-middle Tortonian	10.2[2]	1.45	top Tortonian	7.2[3]	0.7
GA	early Serravallian	13.3[2]	0.3	top Serravallian	11.6[3]	0.3
PM	late Burdigalian	16.7[2]	0.8	top Langhian	13.7[3]	0.4

(B)	Location		Distance (km)		Individual shortening (km)							Cumulative shortening	
Fold	Lon	Lat	D	Err	FM	TE	TB	Symmetric Error		Skewed Error		Avg.	2σ
								a	b	c	d		
OA	12.84	44.04	0.0	1.6	8.0	8.5	0.1	0.1	0.16	0.15	2.05	45.0	3.1
CA	12.76	43.97	11.0	1.6	5.1	4.3	9.4	0.1	0.16	0.15	1.68	39.5	2.8
MA	12.64	43.88	24.5	4.4	5.8	6.9	0.2	0.1	0.16	0.15	1.99	33.2	2.7
OR	12.51	43.77	39.5	2.2	6.9	9.4	14.2	0.1	0.16	0.15	1.80	28.9	2.4
IR	12.40	43.68	53.3	1.7	13.7	15.9	11.0	0.1	0.16	0.15	3.67	18.8	2.1
GA	12.27	43.58	69.8	2.2	0.3	1.2	0.9	0.1	0.16	0.15	0.52	5.3	0.8
PM	12.07	43.42	88.5	3.5	4.7	2.7	6.0	0.1	0.16	0.15	1.04	4.5	0.7

Figure 1

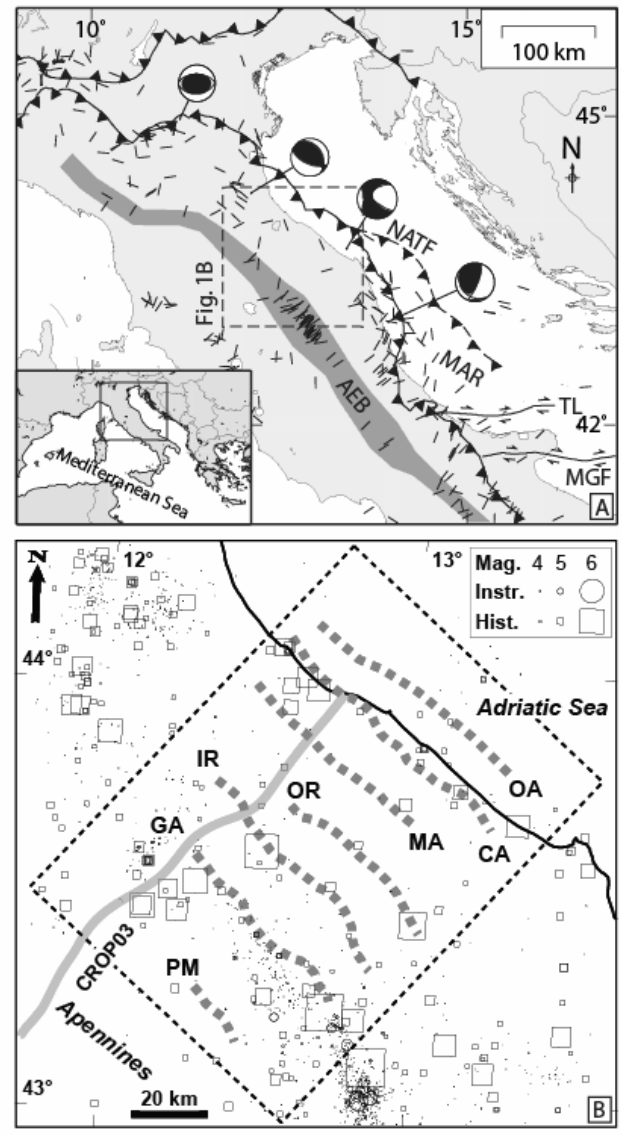
10°
15°
100 km
45°
N
NATF
Fig. 1B
MAR
AEB
TL
42°
MGF
A
Mediterranean Sea
N
12°
13°
Mag. 4 5 6
Instr.
Hist.
44°
Adriatic Sea
IR
OR
OA
GA
MA
CA
CROP03
PM
Apennines
43°
20 km
B

Figure 2

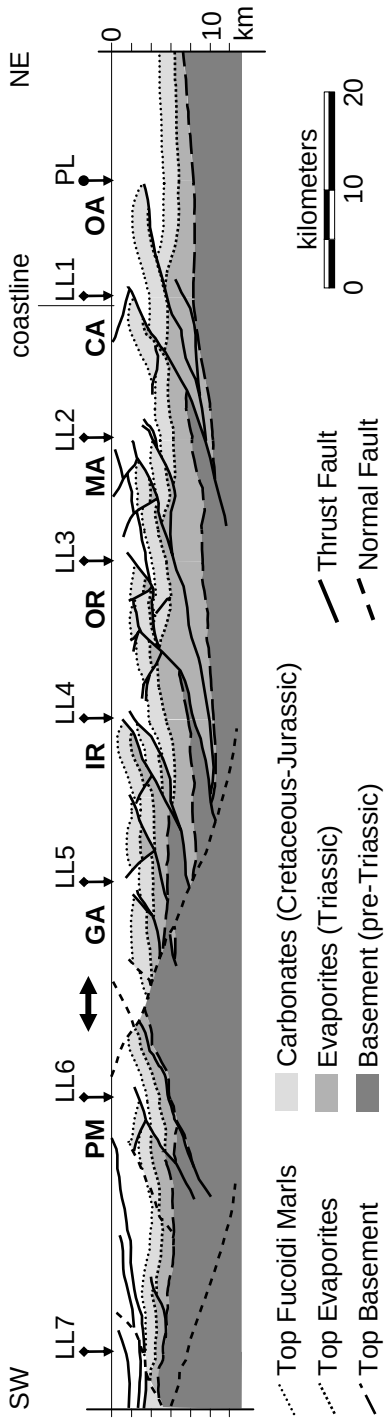
SW
NE
coastline
LL7
LL6
LL5
LL4
LL3
LL2
LL1
PL
PM
GA
IR
OR
MA
CA
OA
0
10
km
kilometers
0
10
20
Top Fucoidi Marls
Top Evaporites
Top Basement
Carbonates (Cretaceous-Jurassic)
Evaporites (Triassic)
Basement (pre-Triassic)
Thrust Fault
Normal Fault

Figure 3

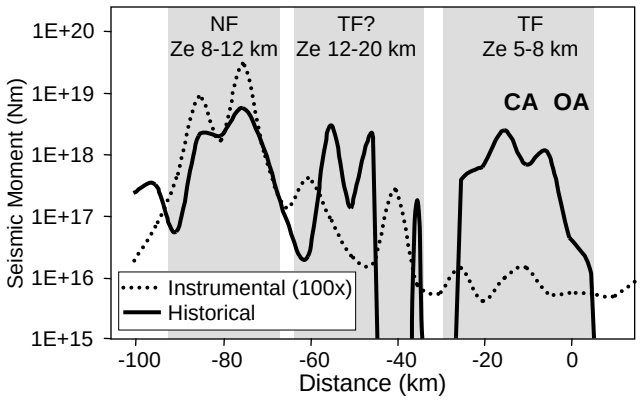
NF
Ze 8-12 km
TF?
Ze 12-20 km
TF
Ze 5-8 km
CA OA
1E+20
1E+19
1E+18
1E+17
1E+16
1E+15
Seismic Moment (Nm)
Instrumental (100x)
Historical
-100
-80
-60
-40
-20
0
Distance (km)

Figure 4

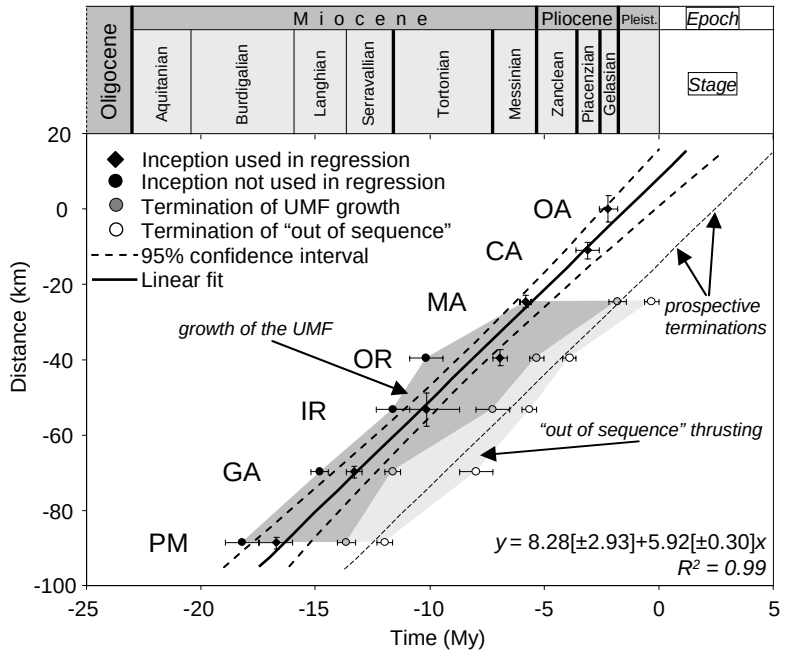
Oligocene
Miocene
Pliocene
Pleist.
Epoch
Aquitanian
Burdigalian
Langhian
Serravallian
Tortonian
Messinian
Zanclean
Piacenzian
Gelasian
Stage
Inception used in regression
Inception not used in regression
Termination of UMF growth
Termination of "out of sequence"
95% confidence interval
Linear fit
OA
CA
MA
OR
IR
GA
PM
growth of the UMF
prospective terminations
"out of sequence" thrusting
y = 8.28[±2.93]+5.92[±0.30]x
R² = 0.99
Distance (km)
Time (My)
20
0
-20
-40
-60
-80
-100
-25
-20
-15
-10
-5
0
5

Figure 5

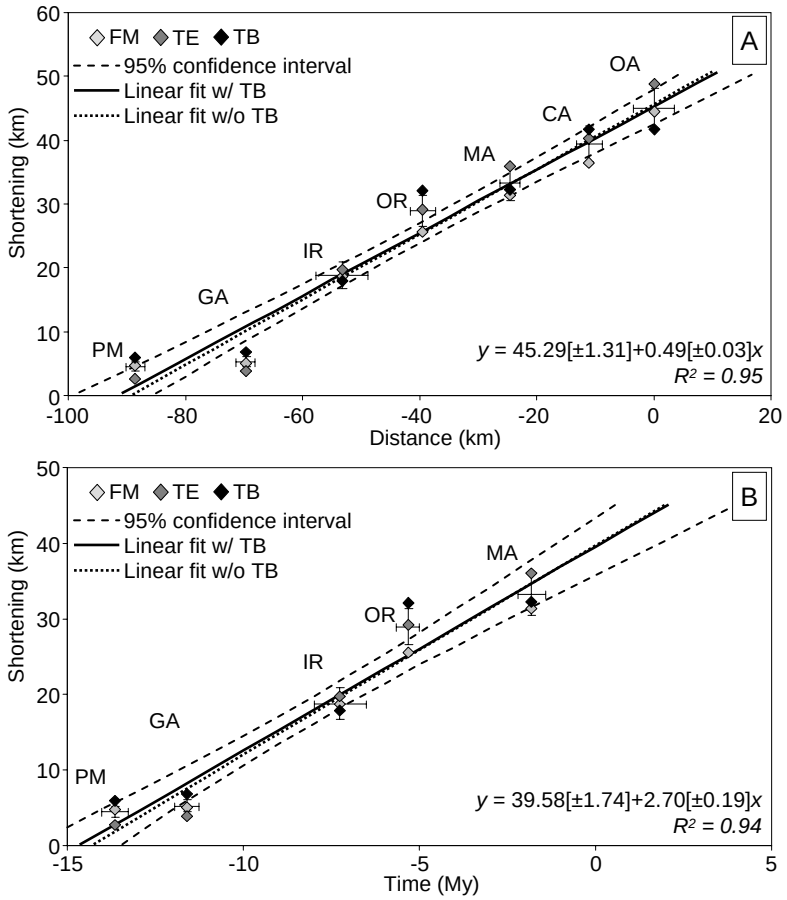
A
FM
TE
TB
95% confidence interval
Linear fit w/ TB
Linear fit w/o TB
OA
CA
MA
OR
IR
GA
PM
y = 45.29[±1.31]+0.49[±0.03]x
R² = 0.95
Shortening (km)
Distance (km)
B
FM
TE
TB
95% confidence interval
Linear fit w/ TB
Linear fit w/o TB
MA
OR
IR
GA
PM
y = 39.58[±1.74]+2.70[±0.19]x
R² = 0.94
Shortening (km)
Time (My)

Figure 6

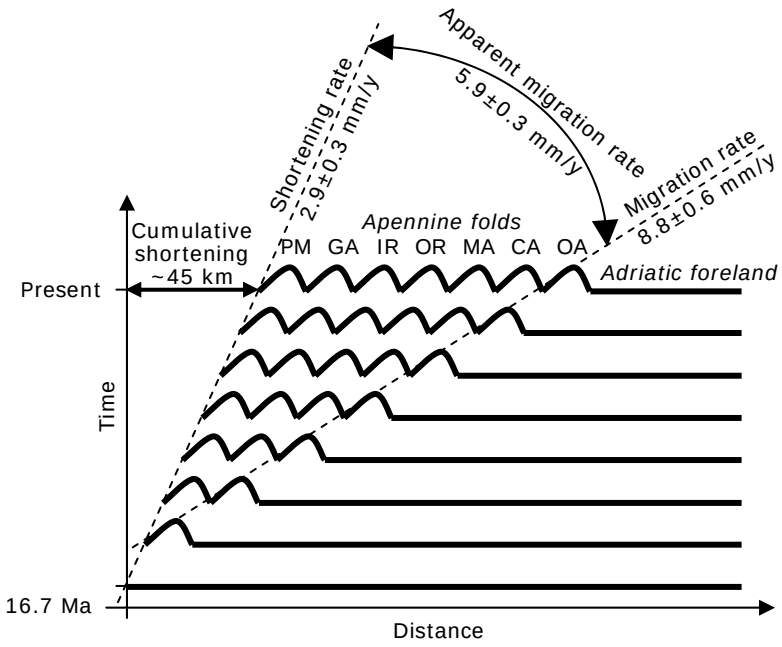
Apparent migration rate
5.9±0.3 mm/y
Shortening rate
2.9±0.3 mm/y
Migration rate
8.8±0.6 mm/y
Cumulative
shortening
~45 km
Apennine folds
PM GA IR OR MA CA OA
Adriatic foreland
Present
Time
16.7 Ma
Distance